JOURNAL OF CATALYSIS 89, 498–510 (1984)

Effects of Metal–Support Interactions on the Chemisorption of H_2 and CO on Pd/SiO_2 and Pd/La_2O_3

ROBERT F. HICKS,[1] QI-JIE YEN,[2] AND ALEXIS T. BELL

Materials and Molecular Research Division, Lawrence Berkeley Laboratory, Department of Chemical Engineering, University of California, Berkeley, California 94720

Received January 31, 1984; revised April 27, 1984

The adsorption of H_2 and CO was investigated on SiO_2- and La_2O_3-supported Pd catalysts, and the structure of adsorbed CO was characterized by infrared spectroscopy. For each of the Pd/SiO_2 catalysts, the ratio of adsorbed H atoms, or adsorbed CO, to surface Pd atoms is unity. The stoichiometry for atomic adsorption of H_2 on Pd/La_2O_3 is also unity, independent of Pd dispersion. By contrast, the adsorption stoichiometry for CO decreases linearly from 0.6 to 0 as the Pd dispersion decreased from 30 to 8%. The suppression of CO adsorption is attributed to patches of partially reduced support material, LaO_x, transferred to the surface of the Pd crystallites during catalyst preparation. The fraction of the Pd crystallite surface covered by LaO_x increases with Pd dispersion, in agreement with conclusions based on earlier XPS studies. Infrared studies indicate that the structures of CO adsorbed on Pd/La_2O_3 and Pd/SiO_2 are similar, but that the strength of adsorption is weaker for Pd/La_2O_3 than for Pd/SiO_2. This is attributed to a weakening in the σ-bond component of the Pd–CO bond due to charge transfer from the LaO_x patches to the Pd crystallites. The absence of any suppression of H_2 adsorption of Pd/La_2O_3 indicates that H_2 adsorption occurs both on the exposed Pd surface atoms as well as on the LaO_x patches covering the balance of the surface Pd atoms.

INTRODUCTION

The synthesis of methanol from CO and H_2 over silica-supported Pd was first demonstrated by Poutsma *et al.* (*1*). Subsequent studies by different investigators (*2–9*) have revealed that the support composition and the presence of promoters can strongly influence both the activity and selectivity of Pd for the synthesis of methanol. Very high specific activities and selectivities to methanol were observed with Pd supported on rare earth oxides, such as La_2O_3 and Nd_2O_3, or with Pd supported on silica promoted with basic metal oxides, such as Na_2O, K_2O, MgO, etc. Conversely, Pd supported on Group IVB metal oxides, such as TiO_2 and ZrO_2, exhibits high specific activity and selectivity for the formation of methane.

The observation that Pd/La_2O_3 catalyzes the synthesis of CH_3OH with both high activity and selectivity motivated us to study the physical and chemical characteristics of this catalyst in greater detail. Our first report on this subject dealt with the characterization of a series of Pd/La_2O_3 catalysts by XPS (*10*). Observations of a series of Pd/SiO_2 catalysts were included in this investigation, so that the results for the Pd/La_2O_3 samples could be compared with those for Pd supported on a "noninteracting" support. The XPS spectra revealed that the chemical state of Pd is affected by an interaction with La_2O_3. In particular, it was found that the Pd $3d_{5/2}$ binding energy lies below that for metallic Pd. The extent of the deviation increased with metal loading, reaching a level of −0.7 eV for 8.8% Pd/La_2O_3. By contrast, the Pd $3d_{5/2}$ binding energy for the Pd/SiO_2 samples was found to be in close agreement with that for bulk Pd, irrespective of the Pd weight loading. The XPS results for Pd/La_2O_3 were rationalized

[1] Present address: Research Division, W. R. Grace & Co., 7379 Route 32, Columbia, Maryland 21044.

[2] Present address: Department of Chemistry, Nanjing University, Nanjing, People's Republic of China.

0021-9517/84 $3.00

in terms of a model which postulates that thin patches of the support partially cover the surface of the Pd crystallites. It was proposed that during reduction of the samples, Pd catalyzes the partial reduction of the patches of La_2O_3 to LaO_x. Because of the electropositive nature of La, the excess electronic charge associated with the LaO is distributed among the surface Pd atoms. A schematic representation of the proposed metal–support interaction is shown in Fig. 1. Here, each patch of LaO_x is assumed to interact with a number of surface Pd atoms (designated as $Pd_{x'}$ in Fig. 1).

The picture of the metal–support interaction illustrated in Fig. 1 is similar in many respects to that recently proposed to explain the strong metal–support interaction (SMSI) produced when Group VIII metals supported on TiO_2 are reduced at elevated temperatures (*11–18*). It is suggested that in the SMSI state, the surface of the metal is covered by small patches of TiO_x which influence the chemical state of the metal and cause a suppression in the chemisorptive capacity of the metal for H_2 and CO (*15–18*). The present study was undertaken to determine whether the patches of LaO_x, believed to be present on the surface of La_2O_3-supported Pd might influence the chemisorption of H_2 and CO. Studies were also carried out with Pd/SiO_2 to establish a basis for comparing the results obtained on Pd/La_2O_3. The relationship of the work reported here to the catalytic properties of Pd/SiO_2 and Pd/La_2O_3 for methanol synthesis will be reported separately (*19, 20*).

EXPERIMENTAL

Catalyst Preparation

All of the catalysts used in this study were identical to those used in the XPS study reported by Fleisch *et al.* (*10*) and were prepared as follows. The Pd precursor, H_2PdCl_4, was obtained by dissolving $PdCl_2$ in concentrated HCl and evaporating until the crystals were dry (*21*). The Pd/La_2O_3 samples were prepared by ion exchanging an aqueous solution of H_2PdCl_4 with $La(OH)_3$. The $La(OH)_3$ (BET surface area, ~11 m^2/g) was obtained by boiling La_2O_3 for 12 hr in distilled water. After ion exchange, the catalyst slurry was held for 12 hr at 338 K; it was then filtered, and the filtrate washed with excess distilled water. The Pd/SiO_2 samples were prepared by incipient wetness impregnation of Cab-O-Sil HS5 silica (BET surface area, 300 m^2/g) with H_2PdCl_4 dissolved in 1 *N* HCl. All samples were dried in a vacuum oven at 338 K, calcined in a 21% O_2/He mixture at 623 K for 2 hr, and reduced in H_2 at 573 K for 3 hr. After reduction, the samples were stored in a desiccator until use in the chemisorption experiments.

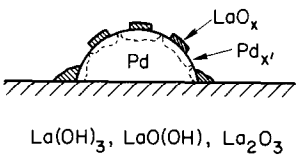

FIG. 1. Schematic illustration of the interaction of Pd with the support.

Catalyst Characterization

The concentration of exposed Pd atoms was determined by H_2–O_2 titration, using the pulsed flow technique (*3, 22–24*). A glass volumetric chemisorption apparatus was used to measure adsorption isotherms for CO and H_2. All samples were reduced in H_2 at 573 K for 1 hr and evacuated at 573 K for 3 hr prior to characterization. Isotherms were obtained at 298 K for pressures ranging from 0 to 250 Torr and were corrected for adsorption on the support. The monolayer coverage of each adsorbate was determined by back-extrapolating the linear portion of the corrected adsorption isotherm to zero pressure (*25*).

The CO adsorption capacity of Pd/SiO_2 and Pd/La_2O_3 at 298 K was also studied by infrared spectroscopy. For these experiments, a catalyst wafer was suspended in an evacuable glass reactor and pretreated as described above. Small doses of CO, approximately one-tenth of a monolayer, were introduced into the reactor, and the

infrared spectrum recorded after each dose. All spectra were collected at 8-cm^{-1} resolution using a Digilab FTS – 10M Fourier-transform infrared spectrometer, equipped with a narrow-band HgCdTe detector. A satisfactory signal-to-noise ratio was obtained by coadding 100 interferograms.

RESULTS

Palladium Dispersion

To measure the Pd dispersion, the catalysts were titrated first with O_2, next with H_2, and then again with O_2. In most experiments, the amount of O_2 consumed initially well exceeded the stoichiometric amounts of H_2 and O_2 consumed in the subsequent two titrations. However, the latter two titrations were always in close agreement with the stoichiometry of two molecules of H_2 per molecule of O_2. The concentration of exposed Pd atoms, C_{Pd_s}, and the Pd dispersion, D_{Pd}, calculated from the results of the H_2 titration and the second O_2 titration, are given for each sample in Table 1.

Both the Pd/SiO_2 and the Pd/La_2O_3 samples exhibit a modest variation in Pd dispersion with Pd weight loading. For Pd/SiO_2, D_{Pd} is nearly constant up to 2.1 wt% Pd, but decreases from 30 to 18% as the loading is further increased to 9.0 wt% Pd. For Pd/La_2O_3, D_{Pd} decreases rapidly from 30 to 8% as the loading increases from 0.25 to 8.8 wt% Pd. The lower Pd dispersion of Pd/La_2O_3 relative to Pd/SiO_2 is probably due to the much lower surface area of the support: 10 to 15 m^2/g for La_2O_3 (*26*), as opposed to 300 m^2/g for Cab-O-Sil HS5 silica.

TABLE 1

Dispersion and Concentration of Exposed Pd Atoms

Catalyst	D_{Pd} (%)	$C_{Pd_s} \times 10^5$ (mol/g)
0.25% Pd/SiO_2	30	0.7
0.75% Pd/SiO_2	28	2.0
2.00% Pd/SiO_2	35	6.5
2.10% Pd/SiO_2	31	6.1
5.10% Pd/SiO_2	26	12.6
9.00% Pd/SiO_2	18	15.3
0.25% Pd/La_2O_3	30	0.7
0.70% Pd/La_2O_3	18	1.2
1.90% Pd/La_2O_3	16	2.9
1.95% Pd/La_2O_3	11	2.1
5.00% Pd/La_2O_3	9	4.1
8.80% Pd/La_2O_3	8	6.9

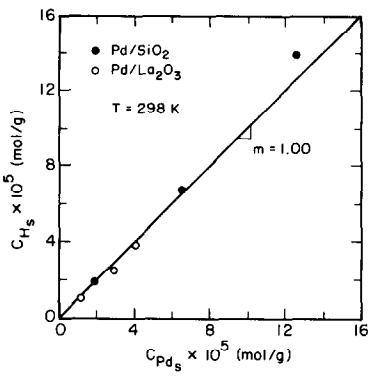

FIG. 2. Correlation of the H_2 adsorption capacity of the Pd/SiO_2 and Pd/La_2O_3 samples with the concentration of surface Pd atoms at 298 K.

H_2 Adsorption

The H_2 adsorption capacity of the catalysts were determined by taking the difference between the total amount of H_2 taken up by adsorption and absorption and that taken up by absorption alone (*22*). The H atom adsorption capacity at 298 K, C_{H_s}, is plotted versus C_{Pd_s} in Fig. 2. The points for SiO_2-supported Pd lie along the diagonal line, indicating that the ratio of adsorbed H-atoms to exposed surface Pd atoms is unity. The points for La_2O_3-supported also lie close to the diagonal, and so there too it is concluded that $C_{H_s}/C_{Pd_s} \simeq 1.0$.

CO Adsorption

The CO adsorption capacity of Pd/SiO_2 at 298 K is plotted versus C_{Pd_s} in Fig. 3. The values of C_{Pd_s} used in the correlation are those determined by H_2–O_2 titration. The concentration of adsorbed CO, C_{CO_s}, is

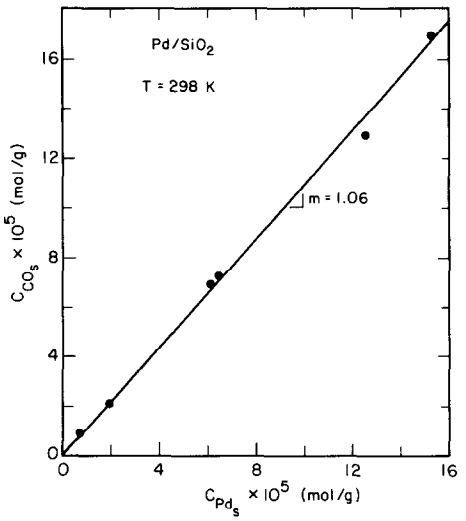

FIG. 3. Correlation of the CO adsorption capacity of the Pd/SiO_2 samples with the concentration of surface Pd atoms at 298 K.

seen to be proportional to C_{Pd_s}. The slope of the line through the data indicates that the number of CO molecules adsorbed per exposed Pd atom is 1.06. Back-sorption isotherms were also measured following a 12-hr evacuation period. Subtraction of the amount of CO back-sorbed form the initial amount adsorbed reduces the stoichiometry to 0.86 CO molecules adsorbed per exposed Pd atom at 298 K.

The CO adsorption capacity of Pd/La_2O_3 at 298 K is plotted versus C_{Pd_s} in Fig. 4. For Pd/La_2O_3, C_{CO_s} does not follow a linear dependence on C_{Pd_s}, nor does the correlation extrapolate through the origin. Instead, the data appear to extrapolate to a nonzero y-intercept, suggesting that there may be some adsorption of CO on the support. It should be noted that in the absence of Pd, La_2O_3 adsorbs very little CO. For example, at $P_{CO} = 200$ Torr the support adsorbs 0.3×10^5 mol/g. Since the amount of CO adsorbed on the support in the absence of Pd has already been subtracted from the data plotted in Fig. 4, the anomolous behavior of the data suggest that the presence of Pd induces additional CO adsorption onto the support.

Infrared Observations of CO Adsorption on 2.0% Pd/SiO₂

Carbon monoxide adsorption at 298 K was studied by infrared spectroscopy, in order to determine the binding sites for CO and to measure the CO adsorption capacity of the exposed Pd. Spectra for CO adsorbed on 2.0% Pd/SiO_2 are shown in Fig. 5. Each spectrum was recorded after adding a fixed dose of CO to the sample chamber containing the catalyst disc. The dosage, X_{CO}, is equal to the moles of CO added per mole of exposed Pd contained within the disk. The infrared spectrum of CO adsorbed on Pd exhibits three bands, located at 2090, 1975, and 1920 cm^{-1}. Following the original assignments of Eischens *et al.* (*27, 28*, the band above 2000 cm^{-1} is attributed to linearly bonded CO, and the bands below 2000 cm^{-1} are attributed to bridge-bonded CO. Hereafter, these bands will be designated L, B_1, and B_2 in order of decreasing vibrational frequency. It should be noted that throughout the addition of CO no other bands appeared in the infrared spectrum from 3200 to 1200 cm^{-1}.

As shown in Fig. 5, the first aliquot of CO, $X_{CO} = 0.13$, causes the L, B_1, and B_2 peaks to appear at 2060, 1960, and 1900

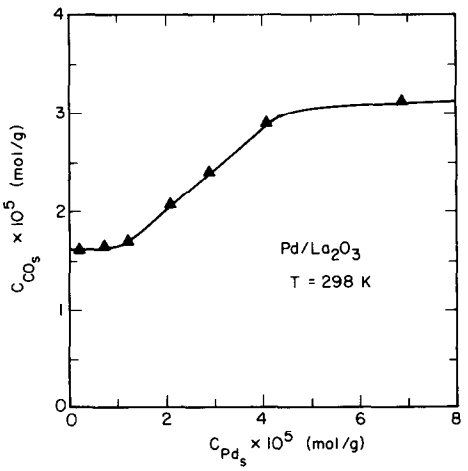

FIG. 4. Correlation of the CO adsorption capacity of the Pd/La_2O_3 samples with the concentration of surface Pd atoms at 298 K.

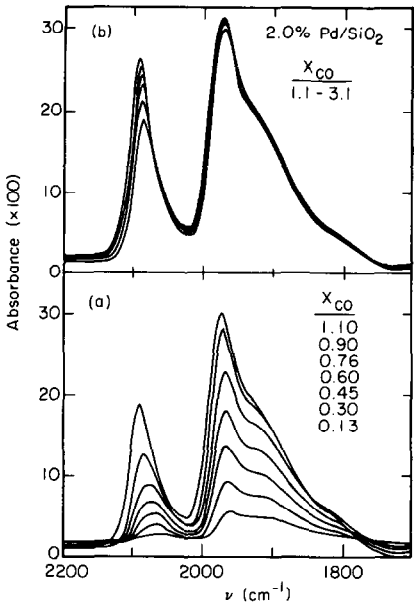

FIG. 5. The infrared spectrum of CO adsorbed on 2.0% Pd/SiO_2 at 298 K: (a) increasing dosages of CO from 0.12 to 1.10 mol CO per mole exposed Pd; (b) increasing dosages of CO from 1.10 to 3.10 mol CO per mole surface Pd.

cm^{-1}, respectively. Addition of more CO leads to a large increase in band intensity with only a modest upscale shift in band frequency: $\Delta\nu_L = 40\ cm^{-1}$, $\Delta\nu_{B_1} = 15\ cm^{-1}$, and $\Delta\nu_{B_2} = 20\ cm^{-1}$. Beyond $X_{CO} = 1.1$, further aliquots of CO do not significantly alter the infrared spectrum. The relatively small shift in frequency with increasing CO uptake indicates that the CO sticking coefficient is high, and, as a consequence, adsorption occurs as a sharp chromatographic front which moves from the exterior to the center of the disk with increasing CO dosage (*29*).

Shown in Fig. 6 is a plot of the integrated absorbance of the infrared spectrum of adsorbed CO versus X_{CO}. The integrated absorbance, $\tilde{A}_T$, is defined as

$$\tilde{A}_T = \frac{\pi R^2 \int_{1600}^{2200} \log_{10}(I/I_0)\, d\nu}{C_{Pd_s} w_c}, \qquad (1)$$

where $\log_{10}(I/I_0)$ is the absorbance, w_c is the weight of the catalyst pellet, and πR^2 is the cross-sectional area of the pellet. A change in the dependence of $\tilde{A}_T$ on X_{CO} above and below $X_{CO} = 1.1$ is clearly evident in Fig. 6. The knee in the curve corresponds to the point at which the Pd surface becomes fully covered by CO, and hence, the value of X_{CO} at the knee is a measure of the CO adsorption stoichiometry, designated X_{CO}^{sat}. The value of $\tilde{A}_T$ at saturation coverage, $\tilde{A}_T^{sat}$, and the value of X_{CO}^{sat} are calculated in the following manner. The plateau region of the curve is back-extrapolated to the y-intercept to determine $\tilde{A}_T^{sat}$. Then, a horizontal line at $y = \tilde{A}_T^{sat}$ is drawn, and the intersection of this line with the curve is used to define X_{CO}^{sat} (see dashed lines, Fig. 6). The application of this method assumes that all the CO added to the sample chamber is adsorbed by the Pd atoms, up to $X_{CO} = X_{CO}^{sat}$. This assumption appears satisfied given the high strength of CO adsorption, and the absence of competing sites for CO adsorption on the support. For 2.0% Pd/SiO_2, the extrapolation technique yields $X_{CO}^{sat} = 1.1$. This value is in excellent agreement with an adsorption stoichiometry of 1.06 determined from the CO adsorption isotherm (see Fig. 3).

The integrated absorption coefficient at saturation $\tilde{A}_T^{sat}$, is determined from

$$\tilde{A}_T^{sat} = \tilde{A}_T^{sat}/X_{CO}^{sat}. \qquad (2)$$

Substituting into Eq. 2 the values of $\tilde{A}_T^{sat}$ and X_{CO}^{sat} obtained from Fig. 6, a value of

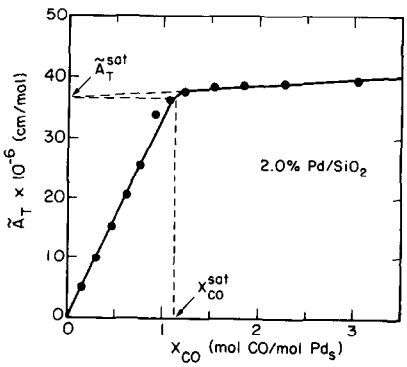

FIG. 6. Correlation of the integrated intensity of the infrared spectrum of CO adsorbed on 2.0% Pd/SiO_2 with CO dosage.

$\bar{A}_T^{sat} = 33.1 \times 10^6$ cm/mol is calculated for the 2.0% Pd/SiO_2 sample. This value is in good agreement with the integrated absorption coefficients for the infrared spectrum of adsorbed CO at high coverages on Ru/SiO_2, Pt/SiO_2, Pd/Al_2O_3, and Pd/SiO_2 (*30, 31*).

Infrared Observations of CO Adsorption on Pd/La_2O_3

The infrared spectrum of adsorbed CO was recorded during CO adsorption on each Pd/La_2O_3 sample at 298 K. Shown in Fig. 7 are a series of spectra for 1.9% Pd/La_2O_3, collected after addition of small amounts of CO. These spectra are characteristic of all of the Pd/La_2O_3 samples. The two bands at 2065 and 1965 cm^{-1} are due to the L and B_1 forms of CO bonded to Pd, respectively, and are quite similar in shape and location to the L and B_1 bands observed for 2.0% Pd/SiO_2. However, in contrast to what is observed for 2.0% Pd/SiO_2, none of the infrared spectra of CO adsorbed on Pd/La_2O_3 evidence a low-frequency shoulder on the B_1 band that would indicate the presence of B_2 adsorption sites. Another distinguishing feature of CO adsorption on Pd/La_2O_3 is that the rapid growth in intensity of the L and B_1 bands with CO dosage stops at dosages which are much less than a monolayer. It is seen in Fig. 7 that for 1.9% Pd/La_2O_3 the L and B_1 bands cease to grow significantly after addition of about 0.37 mol of CO per mole of exposed Pd. It should be noted that the CO dosage at which the infrared bands of adsorbed CO cease to grow is different for each Pd/La_2O_3 sample, and, in fact, for 8.8% Pd/La_2O_3 no infrared bands of adsorbed CO were detected.

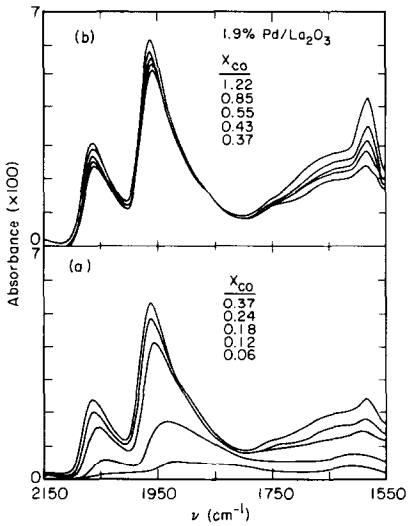

FIG. 7. The infrared spectrum of CO adsorbed on 1.9% Pd/La_2O_3 at 298 K: (a) increasing dosages of CO from 0.06 to 0.37 mol CO per mole exposed Pd; (b) increasing dosages of CO from 0.37 to 1.22 mol CO per mole surface Pd.

Two additional features are found in the infrared spectra of Pd/La_2O_3, which are ascribed to the support. One of these is a broad band extending from 1550 to 1750 cm^{-1}, which is probably due to coordinated water (*32, 33*). Its growth with CO dosage suggests that it is formed by the adsorption and reaction of CO on the support. For example, CO may react with surface hydroxyl groups to form carbonate anions and adsorbed water. The second feature, a sharp peak at 1585 cm^{-1}, is due to the O–C–O stretch of adsorbed formate anion (*6, 34, 35*). The formate anion is also produced by the adsorption and reaction of CO with the hydroxyl groups of the support. This assignment was confirmed by the appearance of the 1585-cm^{-1} band upon exposing a disk of the support to formic acid.

Plots of $\bar{A}_T$ versus X_{CO} are shown in Fig. 8 for five of the Pd/La_2O_3 samples. A curve for 8.8% Pd/La_2O_3 is not shown, since no infrared bands of adsorbed CO were detected for this sample. With the exception of the data for 0.7% Pd/La_2O_3, each of the plots in Fig. 8 exhibits a well-defined knee, similar to that seen in Fig. 6, signifying that adsorption occurs as a chromatographic front which penetrates into the catalyst disk.

Values of X_{CO}^{sat} and $\bar{A}_T^{sat}$ computed from the data shown in Fig. 8 are listed in Table 2. The technique used to obtain these values is the same as that described for Pd/SiO_2 and shown in Fig. 6. It can be seen

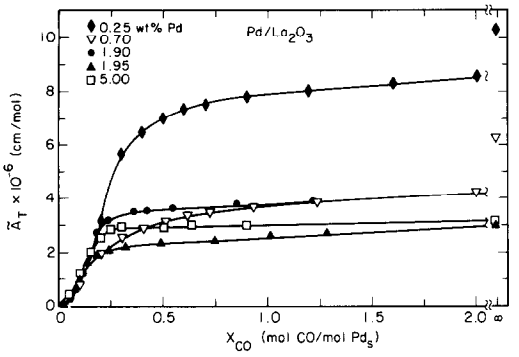

FIG. 8. Correlation of the integrated intensity of the infrared spectrum of CO adsorbed on the Pd/La_2O_3 samples with CO dosage.

from Table 2 that the CO adsorption stoichiometry decreases monotonically with increasing Pd weight loading. This trend is in strong contrast to that observed for the Pd/SiO_2 samples which exhibit a CO adsorption stoichiometry of unity (see Fig. 3). In Fig. 9, X_{CO}^{sat} is plotted versus the Pd dispersion of the Pd/La_2O_3 samples. This figure indicates that the uptake of CO on the Pd decreases with increasing Pd particle size.

The value of $\tilde{A}_T^{sat}$ for the Pd/La_2O_3 samples, given in Table 2, is virtually independent of the Pd weight loading. Thus, a consistent value of the integrated absorption coefficient is obtained, irrespective of the value of X_{CO}^{sat}. It should be noted, however, that the value of $\tilde{A}_T^{sat}$ for Pd/La_2O_3 is a factor of three smaller than that for Pd/SiO_2. The reason for this difference is not fully understood. One possibility is that the gradient of the dipole for CO adsorbed on Pd/La_2O_3 is smaller than that for Pd/SiO_2. Another possibility is that the assumption of a Beer–Lambert relation (Eq. (1)) for Pd/La_2O_3 may not be fully valid, since the large particle size of the La_2O_3 particles ($\sim 1\ \mu m$) results in considerable scattering of the incident radiation (*36*).

The CO adsorption capacity of the support may be estimated by subtracting the uptake on the Pd from the total uptake determined from the CO adsorption isotherm. The CO uptake on the Pd is given by the product of C_{Pd_s} and X_{CO}^{sat}. These values are listed in Table 3 for each of the Pd/La_2O_3 samples. The Pd content of the catalyst is seen to have a strong influence on the amount of carbonate and formate anions formed on the support. From 0.25 to 8.8% Pd, the CO adsorption capacity of the support increases by nearly threefold.

Infrared Observations of CO Desorption

Desorption experiments were carried out in the infrared cell to obtain a qualitative estimate of the strength of the CO bond to Pd supported on both La_2O_3 and SiO_2. A series of infrared spectra of CO adsorbed on 2.0% Pd/SiO_2 and 1.9% Pd/La_2O_3 are

TABLE 2

Spectral Properties of CO Adsorbed on the Supported Pd Catalysts at 298 K[a]

Catalyst	X_{CO}^{sat}	$\tilde{A}_T^{sat} \times 10^{-6}$ (cm/mol)	ν_{CO} (cm^{-1})		
			L	B_1	B_2
2.00% Pd/SiO_2	1.11	33.1	2090	1975	1920
0.25% Pd/La_2O_3	0.60	12.1	2070	1955	—
0.70% Pd/La_2O_3	0.42[b]	10.7	2060	1955	—
1.90% Pd/La_2O_3	0.33	10.3	2060	1960	—
1.95% Pd/La_2O_3	0.22	9.7	2055	1955	—
5.00% Pd/La_2O_3	0.26	10.6	2050	1965	—
8.80% Pd/La_2O_3	0.00	—	—	—	—

[a] Properties are reported for spectra observed at saturation.
[b] Approximate value, estimated by assuming $\tilde{A}_T^{sat} = 10.7 \times 10^6$ cm/mol and $\tilde{A}_T^{sat} = 4.5 \times 10^6$ cm/mol.

TABLE 3

Carbon Monoxide Adsorption Capacity of Pd/La_2O_3 at 298 K

Catalyst	C_{Pd_s}[a]	Pd Uptake[a,b]	La_2O_3 Uptake[a,c]
0.25% Pd/La_2O_3	0.7	0.4	1.2
0.70% Pd/La_2O_3	1.2	0.5	1.2
1.90% Pd/La_2O_3	2.9	1.0	1.4
1.95% Pd/La_2O_3	2.1	0.5	1.6
5.00% Pd/La_2O_3	4.1	1.1	1.8
8.80% Pd/La_2O_3	6.9	0.0	3.2

[a] All values are $\times 10^5$ mol/g.
[b] Pd Uptake = $C_{Pd_s} \times X_{CO}^{sat}$.
[c] La_2O_3 Uptake = $C_{CO_2} - (C_{Pd_s} \times X_{CO}^{sat})$.

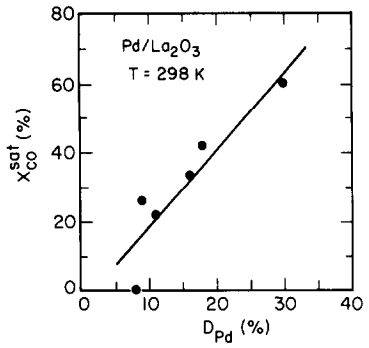

FIG. 9. Correlation of the CO adsorption stoichiometry at 298 K with Pd dispersion for Pd/La_2O_3.

shown in Figs. 10 and 11. These samples were presaturated with a monolayer of CO and then evacuated at progressively higher temperatures. The infrared spectra shown in the figures were recorded after each stage of evacuation. For 2.0% Pd/SiO_2, some CO remains on the Pd surface after evacuating for 1 hr at 573 K, as evidenced by the two infrared bands at 1890 and 1805 cm^{-1}. However, for 1.9% Pd/La_2O_3, all the CO is removed after evacuating for 1 hr at 423 K. These results clearly indicate that the strength of CO adsorption on Pd/La_2O_3 is weaker than that on Pd/SiO_2.

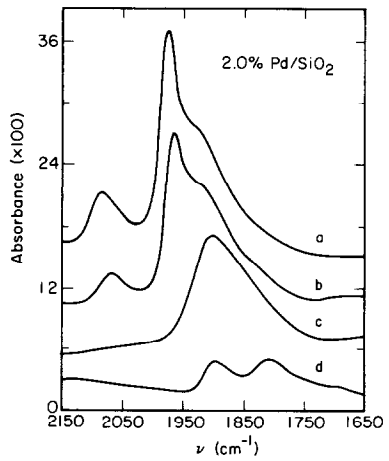

FIG. 10. The infrared spectrum of CO adsorbed on 2.0% Pd/SiO_2 after evacuating (a) 5 min at 298 K, (b) 12 hr at 298 K, (c) 1 hr at 423 K, and (d) 1 hr at 573 K.

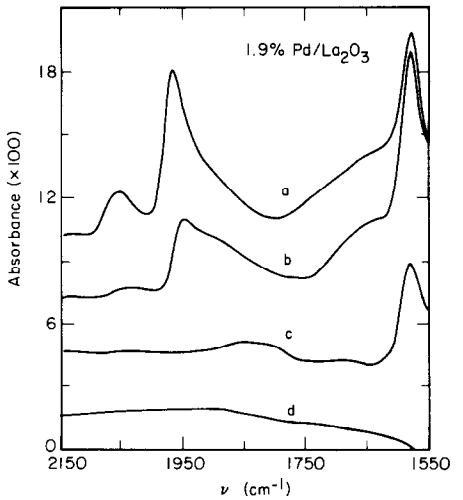

FIG. 11. The infrared spectrum of CO adsorbed on 1.9% Pd/La_2O_3 after evacuating (a) 5 min at 298 K, (b) 12 hr at 298 K, (c) 1 hr at 423 K, and (d) 1 hr at 573 K.

DISCUSSION

Pd Dispersion

The Pd dispersions presented in Table 1 are based on the values of C_{Pd_s} determined by H_2–O_2 titration. While there seems little reason to question the validity of this technique for establishing the dispersions for SiO_2-supported Pd, the question for La_2O_3-supported Pd requires further consideration. The model of the metal–support interaction presented in Fig. 1 envisages a partial coverage of the Pd particles by patches of LaO_x. One must now ask whether the value of C_{Pd_s} measured for the Pd/La_2O_3 catalysts describes the total external surface area of the particle or only that portion of the surface not covered by LaO_x. An answer to this question is provided by the XPS studies reported by Fleisch *et al.* (*10*). These authors showed that the full width-at-half maximum of the Pd $3d_{5/2}$ spectrum for Pd/SiO_2 is identical to that for Pd/La_2O_3, provided both catalysts have the same dispersion as measured by H_2–O_2 titration. Such agreement could only be achieved if the Pd dispersions of the two catalysts are truly the same, and thus, indicates that H_2–O_2 titration provides an accu-

rate measurement of D_{Pd} for Pd/La_2O_3. A further implication of these observations is that the LaO_x species are titrated with the same stoichiometry as the surface Pd atoms. A possible reaction scheme which satisfies this requirement is

1. $PdLaO_x + \frac{1}{2}O_2 \rightarrow PdLaO_{x+1}$
2. $PdLaO_{x+1} + H_2 \rightarrow PdLaO_xH + H_2O$.

The Pd atoms indicated in reactions 1 and 2 are presumed to be those in immediate contact with the LaO_x species.

H_2 Adsorption

For Pd/SiO_2, the ratio of adsorbed H atoms to surface Pd atoms is unity, in close agreement with the results of Boudart and co-workers (*22, 37*). The stoichiometry for hydrogen adsorption on Pd/La_2O_3 is also close to unity, as indicated by Fig. 2. Since, as was discussed above, the value of C_{Pd_s} for La_2O_3-supported Pd includes those Pd atoms covered by patches of LaO_x (see Fig. 1), the observed stoichiometry for hydrogen adsorption suggests that hydrogen will adsorb not only on the exposed Pd atoms, but also on the surface of the LaO_x patches. Evidence for the latter form of adsorption has recently been obtained from TPD studies of H_2 desorption (*38*). It was observed that H_2 desorption occurred both from low-temperature states associated with adsorption on the metal and high-temperature states associated with adsorption on the support. Since the total amount of H_2 desorbed corresponded to a monolayer, based on H_2–O_2 titration, it was concluded that the portions of the support adsorbing H_2 were those covering the Pd particles.

The observations presented here for La_2O_3-supported Pd bear many similarities to those reported recently by Jiang *et al.* (*15*), for TiO_2-supported Ni, NiFe, and Pt in the SMSI state. These authors attribute the manifestations of the metal–support interactions to the presence of TiO_x species on the surface of the metal particles following high-temperature reduction. Nevertheless, hydrogen uptakes determined from desorption measurements were found to provide estimates for metal particle sizes in agreement with sizes determined by X-ray line broadening or transmission electron microscopy. This correlation was attributed to hydrogen adsorption not only on the exposed portions of the metal particles but also at regions of the titania support which are near metal particles or on the TiO_x species which may be present on the surface of the metal particles.

CO Adsorption on Pd/SiO_2

The stoichiometry for CO adsorption on supported Pd has been discussed by several authors (*22, 25, 31, 39*). It has been proposed that at saturation coverage, each linearly bonded CO occupies one adsorption site, whereas each bridge-bonded CO occupies two sites. The results obtained in this study for Pd/SiO_2 strongly suggest that the latter stoichiometry is not correct, and that, in fact, the ratio of bridge-bonded CO to Pd sites is unity. The support for this conclusion comes from the following considerations. All six Pd/SiO_2 samples exhibit a saturation stoichiometry of 1.06 adsorbed CO molecules per surface Pd atom (see Fig. 3). Analysis of the infrared spectrum for CO adsorption at saturation coverage on 2.0% Pd/SiO_2 indicates that 15% of the CO is linearly bonded and 85% is bridge-bonded. If the stoichiometries proposed in the literature were correct, then the overall CO coverage at saturation would have been 0.58, instead of 1.1 as observed. The conclusion that the ratio of bridge-bonded CO to Pd sites is unity can also be drawn from infrared spectra of adsorbed CO on Pd/SiO_2 taken under reaction conditions (*19*). These studies revealed that the distribution of linear- and bridge-bonded CO changes with the weight loading of Pd even though the overall coverage remains at unity. This can only be true if the adsorption stoichiometry of both the linear and bridge forms is one CO per exposed Pd atom.

The B_1 and B_2 bands in the spectrum of CO adsorbed on 2.0% Pd/SiO_2, shown in

Figs. 5 and 11, are quite similar to those reported in the literature for low-dispersion Pd/SiO_2 catalysts prepared from chloride-containing precursors (*29, 40–42*). As was noted in the presentation of Fig. 11, the frequency of the B_1 band shifts from 1975 to 1890 cm^{-1} and the frequency of the B_2 band shifts from 1920 to 1805 cm^{-1} as the CO coverage decreases from unity. Several authors (e.g., (*42, 43*)) have proposed that these bands can be assigned to CO adsorption on Pd(100) and Pd(111) surfaces, based on the similarity of the B_1 and B_2 band positions with those reported by Bradshaw and Hoffmann (*44–46*) for CO adsorption on Pd single-crystal surfaces. Bradshaw and Hoffmann (*44–46*) also demonstrated that coverages as high as 0.82 could be achieved on a Pd(100) surface, and as high as 0.60 on a Pd(111) surface.

The identity of the sites adsorbing CO in a linear fashion is difficult to establish. While studies by Bradshaw and Hoffmann (*44–46*) indicate that linearly adsorbed CO can occur on Pd single-crystal surfaces, studies by other authors suggest that CO adsorption in a linear form can occur on other types of sites. Thus, for example, when Pd is supported in very high dispersion (particle diameters ≤ 15 Å) (*40, 47–49*) or is present in high dilution in a Pd/Ag alloy (*50*), the band for linearly adsorbed CO is found to be exceptionally strong. The conclusion drawn from these observations is that CO can adsorb in a linear form on isolated Pd atoms. A strong band for linearly adsorbed CO has also been reported for CO adsorbed on a polycrystalline Pd foil which has a rough surface (*51*). In this case, the sites for linear adsorption are very likely located at the corners and edges of intersecting crystal planes.

In summary, it appears that bridge-bonded CO can achieve coverages well in excess of 0.5 on the exposed low-index surfaces of both supported and unsupported Pd. Linearly adsorbed CO occurs on Pd atoms located at positions which are not conducive to bridge-bonding. These sites may be in the middle of a crystal plane; at the edges of crystal planes, or at steps, kinks, or other lattice dilocations. Since the L band cannot be resolved into its components, it is not possible to draw definitive conclusions regarding the distribution of linearly bonded CO amongst the different possible sites.

CO Adsorption on Pd/La_2O_3

The infrared–adsorption experiments reveal that CO adsorption at 298 K on Pd/La_2O_3 is suppressed relative to that observed on Pd/SiO_2. As shown in Fig. 9, the CO adsorption stoichiometry, X_{CO}^{sat}, for Pd/La_2O_3 decreases from 0.6 to 0 as the Pd dispersion decreases from 30 to 8%. By contrast, X_{CO}^{sat} for Pd/SiO_2 is 1.1 over a similar range of dispersions. The reduced uptake of CO on Pd/La_2O_3 is very likely due to a blockage of the Pd crystallite surfaces by small patches of support material, as shown in Fig. 1. The decrease in the CO uptake with decreasing dispersion suggests that the blockage of the Pd surface occurs to a greater extent on the large particles.

It is impossible to say from the present experiments how or when patches of La_2O_3 (or LaO_x) are deposited onto the Pd crystallites. One may speculate, however, that the transfer occurs either during the drying of the product formed by the interaction of H_2PdCl_4 with the hydrated support, or upon calcination of the dried material. Raman spectra taken following calcination of the catalyst (*52*) suggest that the Pd is present as both PdO and some mixed metal oxide involving Pd and La. By contrast, Raman spectra of calcined Pd/SiO_2 show only a well-defined peak for PdO.

The apparent increase in the coverage of the Pd crystallites with LaO_x as the dispersion decreases is probably not an intrinsic effect of dispersion. In all cases the lower dispersions occur on catalysts of higher weight loadings. If the transport of support material onto the crystallites is aided in some fashion by chlorine released from H_2PdCl_4 during calcination, then it is easy

to understand why the higher-weight loading catalysts might exhibit higher coverages of the Pd crystallites by LaO_x.

The infrared spectrum of CO adsorbed on reduced Pd/La_2O_3 evidences no unusual binding states of CO, and except for a ~20-cm^{-1} lowering in the vibrational frequencies of all features, the spectrum is very similar in appearance to that seen for Pd/SiO_2. However, infrared observations of CO desorption (see Figs. 10 and 11) reveal that the strength of the metal–carbonyl bond is considerably weaker on Pd/La_2O_3. The weakening of the metal–carbonyl bond is probably due to delocalized charge transfer from the LaO_x patches to the large contiguous areas of the uncovered Pd planes. If the charge transfer was restricted to the immediate vicinity of the LaO_x patches, different binding states of CO should have appeared in the infrared spectrum during CO desorption.

The direction of charge transfer between the LaO_x patches and the Pd surface can be deduced from consideration of the nature of the Pd–CO bond. The bonding of CO involves overlap of a filled carbon 5σ orbital with an empty σ-type orbital on the metal and overlap of a filled $d\pi$ or $dp\pi$ metal orbital with the $2\pi^*$ orbital of CO (*53*). Since Pd has only one unfilled d orbital, charge transfer into or out of this orbital should have a strong affect on the σ-bond. It follows that a weakening in the strength of CO adsorption may be rationalized by charge transfer from the LaO_x to the Pd, thereby filling the metal acceptor orbital and rendering it less capable of σ-bonding. Conversely, since the d orbitals of Pd are nearly filled, charge transfer to the Pd should have a small effect on the π-bonding. The observation of only a ~20-cm^{-1} difference in the C–O stretching frequency for CO adsorbed on Pd/La_2O_3 and Pd/SiO_2 provides evidence that this effect is, indeed, small. Furthermore, a shift to lower frequency for Pd/La_2O_3 indicates that the π-bond is strengthened, most likely as a result of increased charge on the Pd. These considerations, therefore, suggest that the strength of CO adsorption on Pd/La_2O_3 is weakened by charge transfer from the patches of LaO_x to the Pd.

The correlation shown in Fig. 9 suggests that the LaO_x patches cover a greater percentage of the Pd particles with increasing particle size. If it is true that the LaO_x patches transfer charge to the Pd surface, then one might expect to see a parallel increase in the electronegativity of the Pd surface with increasing particle size. Such a trend was observed by XPS (*10*). As the particle size increased, the binding energy for the Pd $3d_{5/2}$ level shifted progressively below that for metallic Pd. Thus, the CO chemisorption results and the XPS results are found to be in good agreement with one another and with the model of the metal–support interaction illustrated in Fig. 1.

The infrared spectra shown in Fig. 7 provide evidence for the adsorption and reaction of CO with the La_2O_3 support to form chemisorbed carbonate and formate anions. Table 3 lists the amount of carbonate and formate that may be produced on La_2O_3 at 298 K. The amount of CO adsorption on the support is not much different than the amount of exposed Pd atoms, and suggests that these adsorption sites are closely associated with the Pd particles. This interpretation is also consistent with the much lower CO adsorption capacity of the support in the absence of Pd.

CONCLUSIONS

The dispersions of SiO_2- and La_2O_3-supported Pd are accurately determined by H_2–O_2 titration. Hydrogen chemisorption of Pd/SiO_2 occurs with a stoichiometry of one H atoms per surface Pd atom. The stoichiometric ratio for adsorbed CO is also unity, regardless of whether CO is linearly or bridge bonded. No variation in the adsorption stoichiometries were observed with changes in the Pd dispersion. The stoichiometry for H_2 adsorption on Pd/La_2O_3 is unity, independent of Pd dispersion, but the stoichiometry for CO decreases linearly

from 0.6 to 0 as the dispersion decreases from 30 to 8%. The suppression of CO adsorption is attributed to patches of LaO_x residing on the surface of the Pd crystallites. The fraction of the Pd crystallite surface covered by LaO_x increases with Pd dispersion, consistent with conclusions drawn previously from XPS studies (*10*). Infrared spectroscopy indicates that the structures of adsorbed CO on Pd/La_2O_3 and Pd/SiO_2 are similar, but the strength of CO adsorption is weaker for Pd/La_2O_3 than for Pd/SiO_2. This is attributed to a weakening in the σ-bond component of the Pd–CO bond due to charge transfer from the LaO_x patches to the Pd crystallites. The absence of any suppression of H_2 adsorption on Pd/La_2O_3 indicates that H_2 adsorption occurs both on the exposed Pd surface atoms as well as on the LaO_x patches covering the balance of the surface Pd atoms. Finally, infrared spectroscopy has revealed that the adsorption of CO to form formate and carbonate species on La_2O_3 is enhanced by the presence of Pd crystallites.

APPENDIX: NOMENCLATURE

$\tilde{A}_T$ integrated absorbance of the infrared spectrum of adsorbed CO, defined by Eq. (3), cm/mol

$\tilde{A}_T^{sat}$ $\tilde{A}_T$ at saturation coverage, cm/mol

$\tilde{A}_I^{sat}$ integrated absorption coefficient of the infrared spectrum of adsorbed CO at saturation coverage, defined by Eq. (4), cm/mol

C_{Pd_s} concentration of exposed Pd atoms, mol/g of catalyst

C_{H_s} concentration of surface H atoms, mol/g of catalyst

C_{CO_s} total CO uptake, mol/g of catalyst

D_{Pd} Pd dispersion

I intensity of the infrared spectrum at a given vibrational frequency

R radius of sample disk, cm

w_c weight of sample disk, g

X_{CO} moles of CO dosed into the sample chamber per mole of exposed Pd atoms on the sample disk

X_{CO}^{sat} X_{CO} at saturation coverage of the sample

ν_i vibrational frequency of species i, cm^{-1}

ACKNOWLEDGMENT

This work was supported by the Division of Chemical Sciences, Office of the Basic Energy Sciences, U.S. Department of Energy under Contract DE-AC03-76SF00098.

REFERENCES

1. Poutsma, M. L., Elek, L. F., Ibarbia, P. A., Risch, A. P., and Rabo, J. A., *J. Catal.* **52,** 157 (1978).
2. Ichikawa, M., *Shokubai* **21,** 253 (1979).
3. Ryndin, Yu. A., Hicks, R. F., Bell, A. T., and Yermakov, Yu. I., *J. Catal.* **70,** 287 (1981).
4. Poels, E. K., van Broekhoven, E. H., van Barneveld, W. A. A., and Ponec, V., *React. Kinet. Catal. Lett.* **18,** 223 (1981).
5. Fajula, F., Anthony, R. G., and Lunsford, J. H., *J. Catal.* **73,** 237 (1982).
6. Kikuzono, Y., Kagami, S., Naito, S., Onishi, T., and Tamaru, K., *Faraday Discuss. Chem. Soc.* **72,** 135 (1982).
7. Ponec, V., *Stud. Surf. Sci. Catal.* **11,** 63 (1982).
8. Poels, E. K., Koolstra, R., Geus, J. W., and Ponec, V., *Stud. Surf. Sci. Catal.* **11,** 233 (1982).
9. Driessen, J. M., Poels, E. K., Hindermann, J. P., and Ponec, V., *J. Catal.* **82,** 26 (1983).
10. Fleisch, T. H., Hicks, R. F., and Bell, A. T., *J. Catal.* **87,** 398 (1984).
11. Tauster, S. J., and Fung, S. C., *J. Catal.* **55,** 29 (1978).
12. Tauster, S. J., Fung, S. C., and Garten, R. L., *J. Amer. Chem. Soc.* **100,** 170 (1978).
13. Tauster, S. J., Fung, S. C., Baker, R. T. K., and Horsley, J. A., *Science* **211,** 1121 (1981).
14. Wang, S.-Y., Moon, S. H., and Vannice, M. A., *J. Catal.* **71,** 167 (1981).
15. Jiang, X.-Zh., Hayden, T. F., and Dumesic, J. A., *J. Catal.* **83,** 168 (1983).
16. Santos, J., Phillips, J., and Dumesic, J. A., *J. Catal.* **81,** 147 (1983).
17. Mériaudeau, P., Dutel, J. F., Dufaux, M., and Naccache, C., *Stud. Surf. Sci. Catal.* **11,** 95 (1982).
18. Resasco, D. E., and Haller, G. L., *J. Catal.* **82,** 279 (1983).
19. Hicks, R. F., and Bell, A. T., *J. Catal.*, in press.
20. Hicks, R. F., and Bell, A. T., *J. Catal.*, in press.
21. Aben, P. C., *J. Catal.* **10,** 224 (1968).
22. Benson, J. E., Hwang, H. S., and Boudart, M., *J. Catal.* **30,** 146 (1973).
23. Freel, J., *J. Catal.* **25,** 139 (1972).
24. Gruber, H. L., *Anal. Chem.* **34,** 1828 (1962).

25. Anderson, J. R., "Structure of Metallic Catalysts." Academic Press, New York, 1975.
26. Rosynek, M. P., and Magnuson, D. T., *J. Catal.* **46,** 402 (1977).
27. Eischens, R. P., Francis, S. A., and Pliskin, W. A., *J. Phys. Chem.* **60,** 194 (1956).
28. Eischens, R. P., and Pliskin, W. A., "Advances in Catalysis," Vol. 10, p. 1. Academic Press, New York, 1958.
29. Palazov, A., Chang, C. C., and Kokes, R. J., *J. Catal.* **36,** 338 (1975).
30. Winslow, P., and Bell, A. T., *J. Catal.*, in press.
31. Vannice, M. A., and Wang, S.-Y., *J. Phys. Chem.* **85,** 2543 (1981).
32. Rosynek, M. P., and Magnuson, D. T., *J. Catal.* **48,** 417 (1977).
33. Klebtsov, P. V., Klebtsova, R. F., and Sheina, L. P., *Zh. Strukt. Khim.* **8,** 270 (1967).
34. Nakamoto, K., "Infrared and Raman Spectra of Inorganic and Coordination Compounds." Wiley, New York, 1978.
35. Edwards, J. F., and Schrader, G. L., *Appl. Spectrosc.* **35,** 559 (1981).
36. Hair, M. L., "Infrared Spectroscopy in Surface Chemistry." Dekker, New York, 1967.
37. Boudart, M., and Hwang, H. S., *J. Catal.* **39,** 44 (1975).
38. Rieck, J. S., and Bell, A. T., unpublished results.
39. Farrauto, R. J., *AIChE Symp. Ser.* No. 143, **70,** 9 (1974).
40. van Hardeveld, R., and Hartog, F., "Advances in Catalysis," Vol. 22, p. 75. Academic Press, New York, 1972.
41. Baddour, R. F., Modell, M., and Goldsmith, R. L., *J. Phys. Chem.* **74,** 1787 (1970).
42. Sheppard, N., and Nguyen, T. T., "Advances in Infrared and Raman Spectroscopy" (R. J. H. Clark and R. E. Hester, Eds.), Vol. 5. Heyden & Sons, London, 1978.
43. Palazov, A., Kadinov, G., Bonev, Ch., and Shopov, D., *J. Catal.* **74,** 44 (1982).
44. Bradshaw, A. M., and Hoffmann, F. M., *Surf. Sci.* **72,** 513 (1978).
45. Ortega, A., Hoffmann, F. M., and Bradshaw, A. M., *Surf. Sci.* **119,** 79 (1982).
46. Hoffmann, F. M., *Surf. Sci. Rep.* **3,** 107 (1983).
47. Clarke, J. K. A., Farren, G., and Rubalcava, H. E., *J. Phys. Chem.* **71,** 2376 (1967).
48. Naccache, C., Primet, M., and Mathieu, M. V., *Adv. Chem. Ser.* **121,** 266 (1973).
49. Figueras, F., Gomez, R., and Primet, M., *Adv. Chem. Ser.* **121,** 480 (1973).
50. Soma-Noto, Y., and Sachtler, W. M. H., *J. Catal.* **32,** 315 (1974).
51. Bradshaw, A. M., and Hoffmann, F. M., *Surf. Sci.* **52,** 449 (1975).
52. Chan, S. S., and Bell, A. T., *J. Catal.*, in press.
53. Cotton, F. A., and Wilkenson, G., "Advanced Inorganic Chemistry." Wiley, New York, 1980.